Applied Radiation and Isotopes 70 (2012) 781–784

Contents lists available at SciVerse ScienceDirect

Applied Radiation and Isotopes

journal homepage: www.elsevier.com/locate/apradiso

Effects of the particle sizes and concentrations on the X-ray absorption by CuO compounds

Roseli Künzel *, Emico Okuno

Universidade de São Paulo, Instituto de Física, Departamento de Física Nuclear, Cidade Universitária, CEP 05508-900, São Paulo, SP, Brazil

ARTICLE INFO

Article history:
Received 4 October 2011
Received in revised form
13 December 2011
Accepted 22 December 2011
Available online 6 January 2012

Keywords:
CuO nanoparticles
X-ray spectroscopy
X-ray absorption

ABSTRACT

This work presents a study on the effects of the particle size, material concentration and radiation energy on the X-ray absorption. CuO nanoparticles and microparticles were incorporated separately into a polymeric resin in concentrations of 5%, 10% and 30% relative to the resin mass. X-ray absorption by these materials was analyzed with a CdTe detector. The X-ray absorption is higher for the nanostructured material compared to the microstructured one for low energy X-ray beams for all CuO concentrations.

1. Introduction

Nanoparticles have become increasingly important in several biomedical applications such as X-ray imaging contrast agents, tumor treatment procedures and in the design of lead-free radiological protection devices (Hainfeld et al., 2006; Cho et al., 2009; Thanh and Green, 2010; Dias et al., 2010; Leung et al., 2011; Botelho et al., 2011). Currently, shielding design of radiological rooms and individual protection equipment of the operating personal under clinical interventional procedures is mainly based on lead materials. These lead protection devices are relatively heavy and the toxicity of this material is also an environmental issue (Scuderi et al., 2006). In this way, new materials, particularly nanostructured compounds due to its good mechanical performance, are being investigated in order to produce lead-free radiological protection devices (Lines, 2008; Moriarty, 2001; Botelho et al., 2011; Scuderi et al., 2006). In this case, the study of the effect of the particle size and concentration on the radiation absorption is necessary which can supply information about the advantages of the use of nanomaterials aiming the replacement of lead based compounds (Botelho et al., 2011; Scuderi et al., 2006; Taylor, 2007).

Recently, the effect of the nanoparticle size on the dose enhancement in radiotherapy has been addressed by Leung et al. (2011) by means of Monte Carlo calculations. These authors performed simulations by considering single nanoparticles with size of 2 nm, 50 nm and 100 nm and observed that the absorbed dose is larger for larger nanoparticle diameters (Leung et al., 2011). According to these authors low energy photon presents a greater probability in interacting with the nanoparticles than the high energy one.

The intensity of transmitted radiation through plates with particles of different sizes incorporated in it has been investigated in several works published in the literature (Berry, 1970; Holynska, 1972). These studies present results relative to grain size in the range between 30 μm and 300 μm. According to the results presented by Holynska (1972), the grain size effect decreases significantly with the increase of the energy of absorbed radiation. Botelho et al. (2011) compared the X-ray absorption by microsized and nanosized materials for 5% concentration of CuO in beeswax. According to these authors, the nanosized materials absorb more radiation when exposed to low energy X-ray beam than the microsized ones. For high energy X-rays beams, specifically X-ray beams generated at 60 and 102 kV tube voltages, the absorption by both materials was similar. However, the effect of CuO particles' concentration in the dispersion media and a detailed spectroscopic analysis was not addressed by these authors.

In this study we have employed a CdTe detector to measure the transmitted X-ray spectra through CuO composites of microsized and nanosized materials as a function of the particles' concentration in a polymeric resin, X-ray beam energy and sample thickness. We used a CdTe detector to register the transmitted X-ray beams through the samples because this system presents good energy resolution in the diagnostic energy range (Miyajima, 2003; Abbene et al., 2010; Künzel et al., 2006).

* Corresponding author. Tel.: +55 1130916975.
E-mail address: roselikunzel@gmail.com (R. Künzel).

0969-8043/$ - see front matter © 2011 Elsevier Ltd. All rights reserved.
doi:10.1016/j.apradiso.2011.12.040

The corrected X-ray spectra and the air kerma values calculated from these beams were used to evaluate the effect of the aforementioned parameters on the X-ray absorption.

2. Materials and methods

2.1. Samples production

In this work, CuO nanoparticles with grain size in the range between 10 and 100 nm, produced by Brasilian Industry Nanum, and CuO microparticles (Vetec Química Fina, Brazil) with 56 μm average particle size were incorporated in an epoxy resin in proportions of 5%, 10% and 30%, relative to the resin mass. The materials were produced with an epoxy resin, CuO powder and a curing agent. In this work the cure agent was Tri-ethylene tetramine which was added to the mixture in a proportion of 10% relative to the resin mass. All the mixture components were weighed with an accuracy of 0.01 g by a calibrated balance. The samples were prepared as follows: (a) careful mixing of resin, CuO powder and curing agent and pouring out on a cylindrical silicon device; (b) drying at room temperature for about 24 h; (c) sanding and polishing the plates and (d) measurement of the plates thickness with a calibrated micrometer. Following these procedures, plates with about 2 cm radius and thickness between 3 and 9 mm were produced for both microsize and nanosize CuO particles in the proportions specified above.

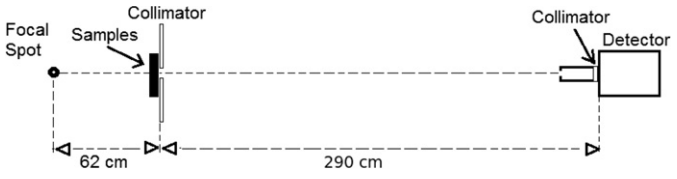

Fig. 1. Experimental setup used in the measurements of the transmitted X-ray spectra through the materials.

2.2. X-ray spectroscopy

The knowledge of the transmitted X-ray spectra through a given material provides important information about the radiation absorption by its components as a function of the photon beam energy. In this work the X-ray beams were emitted by a Philips equipment MG 450 model, connected to a constant potential generator. This tube has a Be window of 2.2 mm thickness with a fixed tungsten anode tube (22° anode angle). The radiation beams were detected by a XR-100T-CdTe detector (Amptek, Inc., Bedford, MA) with 9 mm^2 nominal active area and 1 mm nominal thickness. Output pulses were processed by a Digital Pulse Processor (DPP) PX4. The detector is cooled by Peltier cells and has a 100 μm Be window. An EXVC tungsten Collimator Housing with a 1000 μm aperture and 2 mm thickness was used in front of the detector. The energy calibration of the spectrometer was performed using the measured spectra of gamma-rays and X-rays emitted by ^{241}Am, ^{133}Ba and ^{152}Eu radioactive sources.

Fig. 1 presents a schematic setup of the experimental arrangement used in the spectra measurements. Transmitted spectra through the samples have been registered with the detector positioned in the center of the radiation field at a distance of 352 cm from the focal spot. A lead collimator with aperture of 1.6 cm has been positioned after the sample at a distance of 62 cm from the focal spot. Alignment between the focal spot and CdTe detector was performed with a laser device. The transmitted X-ray spectra were registered for 25, 30, 60 and 120 kV tube voltages. Pile-up rejection and Rise Time Discriminator (RTD) were switched on in the DPP system. Pile-up were maintained at less than 2% during the spectrum acquisition procedures.

The experimental spectra measured with CdTe detector were corrected for all possible interactions of incident photons with

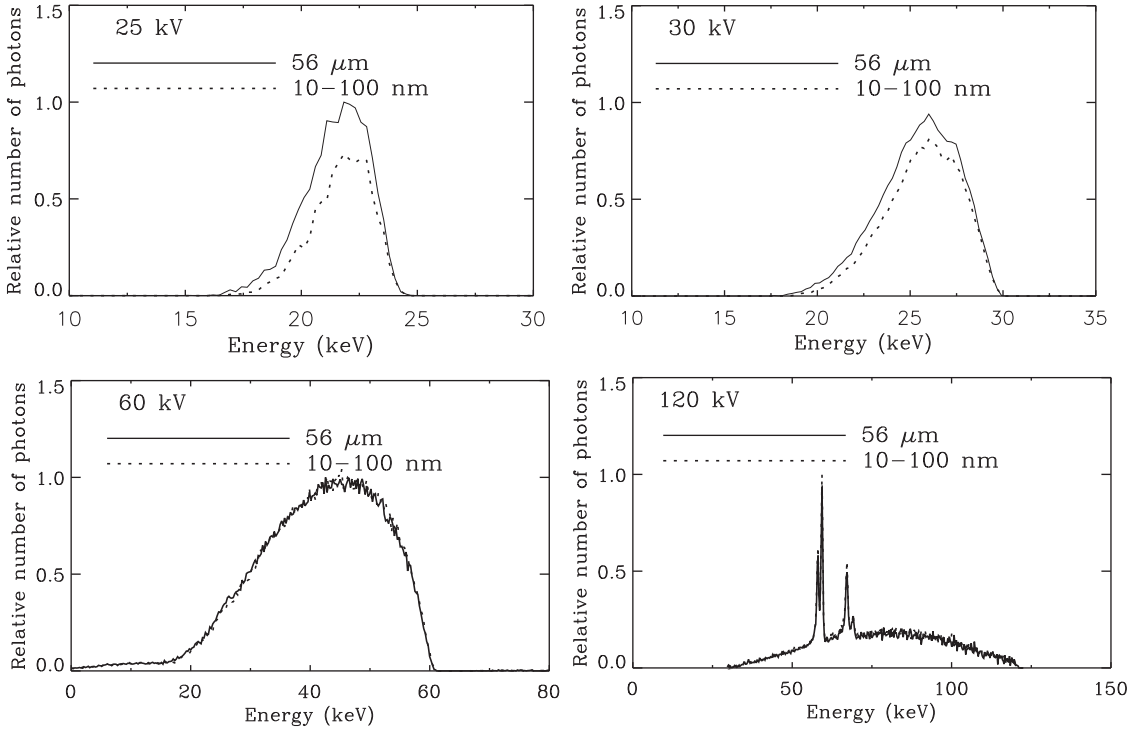

Fig. 2. X-ray spectra transmitted through 10.3 mm samples composed of 30% CuO incorporated to a polymeric resin. Data were recorded for beams generated at 25, 30, 60 and 120 kV tube voltages. Solid lines stand for the microstructured material whereas the dashed ones correspond to the nanostructured samples.

partial deposition of their energy in the detector (Miyajima, 2003; Künzel et al., 2004, 2006). The air kerma for photons with energy E was calculated as follows (Johns and Cunningham, 1983):

$$K_{air}(E) = \Phi(E)E(\mu_{en}/\rho)_{air}(E) \quad (1)$$

where μ_{en}/ρ corresponds to the air mass-energy absorption coefficient (Berger et al., 2005). The quantity $\Phi(E)$ (photons/mm^2) is the photon fluence and E, the photon energy. Total air kerma was calculated by the integration of the air kerma spectra over the whole energy range. After the calculation of the air kerma for all material thicknesses, for a given CuO concentration and beam energy, an exponential interpolation was used to obtain K_{air} values for the nanosized and microsized compound for the same thicknesses. The ratio between the air kerma values for the microstructured and nanostructured materials was calculated as

$$K_\mu/K_n = \frac{(\int_{E_{min}}^{E_{max}} K_{air}(E)\,dE)_{microsize}}{(\int_{E_{min}}^{E_{max}} K_{air}(E)\,dE)_{nanosize}} \quad (2)$$

where E_{min} and E_{max} correspond to the minimum and the maximum energies of the corrected X-ray spectra, respectively.

3. Results and discussion

The X-ray spectra transmitted through (10.3 ± 0.3) mm thickness plates composed of 30% nanostructured CuO powder and 30% microstructured CuO powder, both relative to the resin mass, are illustrated in Fig. 2. The incident X-ray beams on the samples were absorbed only by the inherent X-ray tube filtration. No additional filtration was used in front of the X-ray tube. In Fig. 2 the transmitted X-ray beams spectra through the microsized material were normalized to unity at the maximum of the spectra. The normalization of the transmitted X-ray beams through the nanosized material was performed using the normalization factor of the corresponding spectra transmitted through the microsized sample. The comparison of the relative number of photons for each measured spectra at 25 and 30 kV tube voltages reveals that the nanostructured material absorbs more low energy photons relative to the microstructured ones. Results also show that the larger difference in the X-ray absorption by these materials is due to the beam generated at 25 kV tube voltage. At 30 kV tube voltage the difference between the X-ray absorption by nanosized and microsized materials CuO materials decreases. For the X-ray beams produced at 60 and 120 kV tube voltages, a minimal difference, less than 2%, in the X-ray transmission through the nanostructured and microstructured materials is observed.

Fig. 3 depicts the data relative to the ratio $(K_\mu/K_n)_{air}$ registered for 5%, 10% and 30% CuO powder concentration into an epoxy resin, relative to the resin mass, for 25, 30 and 60 keV maximum X-ray beams energy. Results show that for all the CuO concentrations into the resin, the X-ray beam generated with a maximum energy of 60 keV, this ratio remains about 1.0 over all materials thickness range. On the other hand, the transmission measured at 25 kV tube voltages indicates that the nanostructured material absorbs more radiation than the microstructured one and the ratio $(K_\mu/K_n)_{air}$ ranges between about 1.0 and 1.10 for 5% CuO concentration and material thickness between 5 and 15 mm, 1.35 to 1.6 for 10% CuO concentration and thickness between 8 and 20 mm and 1.2 to 1.5 for 30% CuO concentration and thickness between 3 and 10.3 mm. The values determined for $(K_\mu/K_n)_{air}$ for 25 kV X-ray beams give an indication that the nanostructured samples absorb more low energy radiation than the microstructured ones. For example, the values of the ratio $(K_\mu/K_n)_{air}$, measured from the transmitted spectra through samples produced with 30% CuO powder concentration in the resin, and

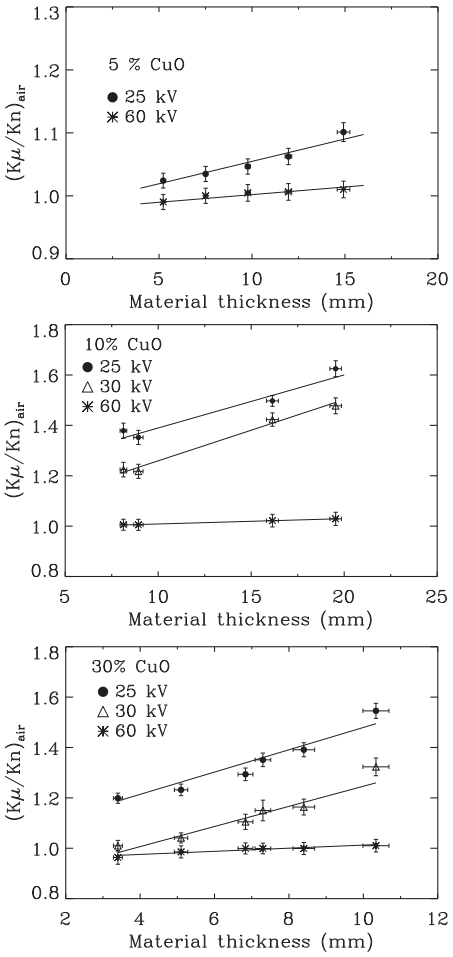

Fig. 3. Ratio of the air kerma values calculated from the transmitted spectra through the microstructured and the nanostructured samples with CuO powder concentration of 5%, 10% and 30% incorporated into the resin.

material thickness between 3 and 10.3 mm, show that K_n ranges from $0.84K_\mu$ to $0.67K_\mu$, which represents a difference in the air kerma values between 16% and 33%.

In the case of the X-ray beams emitted with a maximum energy of 30 keV the values of $(K_\mu/K_n)_{air}$ are in the range between 1.2 and 1.5 for materials' thickness ranging from 8 to 20 mm and 10% CuO concentration relative to the resin mass and between 1.0 and 1.3 for material thickness from 3 to 10 mm and 30% CuO powder concentration in the epoxy resin.

Comparing the results presented in Fig. 3 for 5%, 10% and 30% CuO powder concentration in the resin, one can observe that the grain size effect increases with the increase of the material thickness for low energy X-ray beams. For higher energy X-ray beams, namely those measured for 60 kV tube voltages, the effect of the grain size remains unchanged over the material thickness and concentration studied in this work.

Fig. 4 presents a comparison among the variation of the ratio $(K_\mu/K_n)_{air}$ with the material concentration and X-ray beam maximum energy. Data were interpolated for the same materials' thickness. Results show that for the X-ray beams measured at 25 kV tube voltages the effect of the grain size enhances with the increase of CuO concentration in the resin. For higher energy beams the X-ray transmission through nanosized and microsized materials is about the same for the materials' concentrations studied in this work.

Fig. 5 displays the dependency of the air kerma values with the nanostructured CuO concentration in the resin. Air kerma values

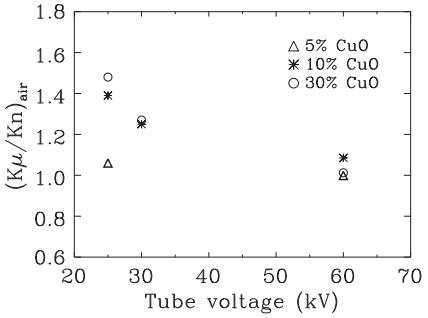

Fig. 4. Illustration of the ratios of air kerma values measured for X-ray beams generated at 25, 30 and 60 kV tube voltages and transmitted through the nanosized samples with 5%, 10% and 30% CuO powder concentration in an epoxy resin.

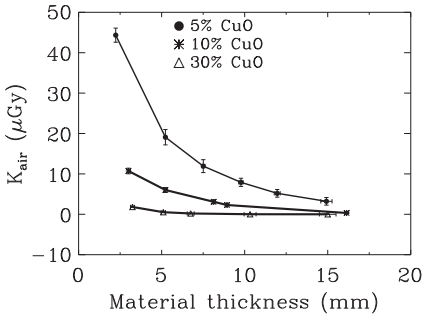

Fig. 5. Illustration of the air kerma values measured for X-ray beams generated at 25 kV tube voltages transmitted through samples with 5%, 10% and 30% CuO powder incorporated in an epoxy resin.

were normalized by the mAs used in the X-ray spectra measurements. Results show that the air kerma are higher for lower CuO concentration in the resin.

Results presented in this work demonstrate that the effect of the particle size in the X-ray absorption depends mainly on the X-ray beam energy. For low energy photons, the effect of the particle size is more evident than for higher energy X-ray beams. Besides, due to the difference on the particle size between the microstructured and nanostructured materials, the number of particles also changes between these composites for a same CuO concentration, per mass, in the resin. As the particle size decreases, the number of particles increases. Regarding the particle sizes used in this work, one microparticle is equivalent in scale to about 600 nanoparticles. Therefore, the distribution of the nanoparticles in the resin should also be different from that presented by the microparticles, resulting in a more uniform dispersion in the resin. This effect can also be responsible for the higher absorption of the low energy X-ray photons by the nanostructured CuO material when compared to the same proportion of CuO material but with microsized particles.

4. Conclusion

Results show that the ratio between the air kerma calculated from the X-ray spectra transmitted through the microstructured samples and those transmitted through the nanostructured material for X-ray beams generated at 60 kV tube voltage remained mostly unchanged over all material thickness range and concentration studied in this work. On the other hand, for beams generated at 25 and 30 kV, the values of the ratio $(K_\mu/K_n)_{air}$ increase with the increase of the sample thickness for all material concentrations studied in this work. Results show that the nanosctructured CuO samples present a greater potential in absorbing low energy X-ray photons compared to the samples produced with microstructured CuO. Therefore, the data presented in this work suggest that a nanostructure-based radiological protection device reduces the radiation dose in the same proportion or even more than devices designed with the same material in its microstructured form.

Acknowledgments

The authors thank the Brazilian Agency Fapesp (Fundação de Amparo a Pesquisa do Estado de São Paulo) through Process 2010/06814-4 and CNPq (Conselho Nacional de Desenvolvimento Científico e Tecnológico).

References

Abbene, L., Gerardi, G., Del Sordo, S., Raso, G., 2010. Performance of a digital CdTe X-ray spectrometer in low and high counting rate environment. Nucl. Instrum. Methods: Phys. Res. A 621, 447–452.

Berger, M.J., Hubbell, J.H., Seltzer, S.M., Chang, J., Coursey, J.S., Sukumar, R., Zucker, D.S., Olsen, K., 2005. XCOM: Photon Cross Section Database (version 3.1). National Institute of Standards and Technology, Gaithersburg, MD. Available online : 〈http://physics.nist.gov/xcom〉.

Berry, P.F., 1970. Particle size heterogeneity phenomena in X-ray analysis. In: Proceedings of the Third Symposium of Low Energy X- and Gamma Ray Sources and Applications, Boston College, Massachusetts.

Botelho, M.Z., Kunzel, R., Okuno, E., Levenhagen, R.S., Basegio, T., Bergmann, C.P., 2011. X-ray transmission through nanostructured and microstructured CuO materials. Appl. Radiat. Isot. 69, 527–530.

Cho, S.H., Jones, B.L., Krishnan, S., 2009. Dosimetric feasibility of gold nanoparticle-aided radiation therapy (GNRT) via brachytherapy using low energy Gamma-/X-ray sources. Phys. Med. Biol. 54 (16), 4889–4905.

Dias, A.L., Künzel, R., Levenhagen, R.S., Okuno, E., 2010. Application of computed tomography images in the evaluation of magnetic nanoparticles biodistribution. J. Magn. Magn. Mater. 322, 2405–2407.

Hainfeld, J.F., Slatkin, D.N., Focella, T.M., Smilowitz, H.M., 2006. Gold nanoparticles: a new X-ray contrast agent. Br. J. Radiol. 79, 248–253.

Holynska, B., 1972. Study of the effect of grain size heterogeneity in the X-ray absorption analysis of simulated aqueous slurries. Spectrochim. Acta 27B, 237–245.

Johns, H.E., Cunningham, J.R., 1983. The Physics of Radiology, 4th ed. Charles C. Thomas Publishers, Springfield.

Künzel, R., Herdade, S.B., Costa, P.R., Terini, R.A., Levenhagen, R.S., 2006. Ambient dose equivalent and effective dose from scattered X-ray spectra in mammography for Mo/Mo, Mo/Rh and W/Rh anode/filter combinations. Phys. Med. Biol. 51, 2077–2091.

Künzel, R., Herdade, S.B., Terini, R.A., Costa, P.R., 2004. X-ray spectroscopy in mammography with a silicon PIN photodiode with application to the measurement of tube voltage. Med. Phys. 31 (11), 2996–3003.

Leung, M.K.K., Chow, J.C.L., Chithrani, B.D., Lee, M.J.G., Oms, B., Jaffray, D.A., 2011. Irradiation of gold nanoparticles by x-rays: Monte Carlo simulation of dose enhancements and the spatial properties of the secondary electrons production. Med. Phys. 38, 624–631.

Lines, M.G., 2008. Nanomaterials for practical functional uses. J. Alloys Compd. 449, 242–245.

Miyajima, S., 2003. Thin CdTe detector in diagnostic X-ray spectroscopy. Med. Phys. 30 (5), 771–777.

Moriarty, P., 2001. Nanostructured materials. Rep. Prog. Phys. 64, 297–381.

Scuderi, G.J., Brusovanik, G.V., Campbell, D.R., Henry, R.P., Kwone, B., Vaccaro, A.R., 2006. Evaluation of non-lead-based protective radiological material in spinal surgery. Spine J. 6, 577–582.

Taylor, E.W., 2007. Organics, polymers and nanotechnology for radiation hardening and shielding applications. SPIE 6713 (671307), 1–10.

Thanh, N.T.K., Green, L.A.W., 2010. Functionalisation of nanoparticles for biomedical applications. Nano Today 5, 213–230.